Polymer Science

Morphological changes in SBS block copolymers caused by oil extension as determined by absolute small angle x-ray scattering

S. Polizzi, N. Stribeck, H. G. Zachmann, and R. Bordeianu[1])

Institut für Technische und Makromolekulare Chemie der Universität Hamburg, Hamburg, F.R.G.
[1]) ICECHIM Bucharest, Romania

Abstract: A series of SBS block copolymers diluted with different amounts (0–60 wt%) of three different kinds of oil were investigated: 1) lithene PM (a low molecular weight polybutadiene); 2) a paraffinic mineral oil with its electron density close to that of the polybutadiene (PB) phase; 3) a highly aromatic mineral oil with an electron density close to the polystyrene (PS) phase. All the oils seem to go into the polybutadiene matrix. Paraffinic oil and lithene form a homogeneous phase with PB; the aromatic oil at low concentrations mixes with the PB phase with a high level of inhomogeneity, while at higher concentration partial phase separation occurs. In the undiluted polymer, styrene forms cylinders in hexagonal packing. The distance between cylinders (about 43 nm) is not significantly changed upon dilution up to 33 wt%. Previously proposed changes in the morphology of PS domains at larger oil contents can be related to observed changes in the long period, in the segment length distributions, and in the homogeneities of the phase (density fluctuations). The electron density difference obtained for pure SBS is lower than the theoretical one calculated from the densities of pure PS and pure PB. Dilution by paraffinic oil improves the phase separation.

Key words: Block copolymers, oil dilution, morphology, phase separation, phase homogeneity, absolute SAXS.

1. Introduction

Tri-block copolymers of the SBS-type are typical two-phase systems, one phase being formed by polystyrene (PS) and the other by polybutadiene (PB). When the fraction of PS in the polymer is not too large, thermoplastic rubbers are obtained. These materials are sometimes diluted with mineral oils in order to improve the injection molding behavior and the properties of the material [1]. Earlier investigations of the mechanical behavior [2, 3] indicated that the oil mainly invades the PB phase and does not form a third phase, so that we should also find a two-phase system for the diluted samples. Furthermore, it was suggested that for large oil contents a morphological transition takes place. The shape of the curve showing the tensile modulus vs volume of rubber can be fitted under the assumption that the rigid particles forming the network change their shape from an elongated to a more spherical one, when the oil fraction exceeds a critical value.

Structure investigations of such materials are of special interest. In the case of the undiluted copolymer, it has been found by electron microscopy that the PS forms cylinders, spheres, or lamellae which are arranged regularly in the PB matrix. Such structures have been confirmed by small angle x-ray scattering (SAXS) [4, 5]. No such systematic structure investigations have been presented for copolymers extended with mineral oils.

In the present investigation we report some results concerning the influence of different oils on the structure of the SBS block copolymer as determined by absolute SAXS.

2. Theoretical section

For a complete evaluation of the SAXS curves, the absolute intensity of the scattering in electron units has to be measured. Such measurements can be performed either by using a reference sample [6] or by a direct

measurement of the primary beam intensity using the moving slit method [7] and taking into account all geometrical factors as well as the x-ray absorption by the sample. The latter method was used in the present work. In this case, as can be shown (see appendix), the smeared absolute scattered intensity per unit volume, $J(\mathbf{s})/V$, is given by

$$\frac{J(\mathbf{s})}{V} = \frac{r_R}{t \cdot e^{-\mu t} \cdot H \cdot L \cdot \lambda \cdot r_e^2} \cdot \frac{P_R(\mathbf{s})}{P_o} \tag{1}$$

where $P_R(\mathbf{s})$ is the power of the scattered x-ray beam measured by the detector with a slit opening of $H \times L$ in the plane of registration, r_R the distance between the sample and the plane of registration, t the thickness, $e^{-\mu t}$ the absorption of the sample, λ the wavelength of the radiation, r_e is Thomson's classical electron radius and P_o the primary beam power per unit slit length in the plane of registration; $\mathbf{s}$ is the scattering vector with $|\mathbf{s}| = s = (2 \sin \Theta)/\lambda$, Θ being half of the scattering angle.

An important quantity is the scattering power Q (or Porod's invariant). If the slit is considered to be of "infinite length", as in our case, Q is obtained from the smeared intensity $J(s)$ by means of

$$Q = \frac{2\pi}{V} \int_0^\infty s J(s)\, ds\,. \tag{2}$$

In the case of an ideal two-phase system with sharp transitions between the two phases and a uniform electron density in each phase, Q is related to the volume fractions v and $(1-v)$ of the two phases and to the difference in their electron densities, $(\varrho_2 - \varrho_1)$, by the following equation

$$Q_{id} = v(1-v)\,(\varrho_2 - \varrho_1)^2\,. \tag{3}$$

Thus, by measuring Q_{id} the electron density difference, $(\varrho_2 - \varrho_1)$, can be determined if v is known, and vice versa.

Without any further a priori assumption of a model for the superstructure, the topology of the considered ideal two-phase system can be described by the segment length distribution [8–10] $n(r)$ obtained from the scattering curve by means of the equation

$$n(r) = \frac{\pi}{2 l_p} \int_0^\infty \tilde{G}_{id}(s) \cdot J_0''(2\pi r s)\, ds \tag{4}$$

with

$$\tilde{G}_{id}(s) = 16\pi^2 [s^3 J_{id}(s) - \lim_{s\to\infty} (s^3 J_{id}(s))]\,. \tag{5}$$

$J_{id}(s)$ is the smeared scattering intensity of the ideal two-phase system and $\lim (s^3 J_{id}(s))$ represents the Porod asymptote A_p. $\tilde{G}_{id}(s)$ is called the interference function. J_0'' is the second derivative (with respect to the $2\pi rs$) of the Bessel function of order 0. l_p is the mean chord length of the two-phase system. If, as in our case, the particles in the two-phase system are not diluted, the interpretation of $n(r)$ is rather complicated. In any case, the maximum of the first peak in $n(r)$ is close to the most probable distance between neighboring phase boundaries in the sample.

The assumption of an ideal two-phase system is always an approximation. In reality, there exist short range electron density fluctuations within each of the two phases, which lead to an additional background scattering, $J_{Fl}(s)$. One also has to assume a transition zone between the two phases, which can be characterized by a thickness d_z. This leads to deviations from Porod's law, according to which, at large scattering angles, $J(s)$ decreases proportionally to $1/s^3$. For a correct evaluation one has to determine $J_{Fl}(s)$, d_z, and the scattering curve of the corresponding ideal two-phase system, $J_{id}(s)$. This is done in the present work by the procedure developed by Ruland et al. [11–14], briefly discussed in the following.

For polymers, at intermediate angles between SAXS and WAXS the main contribution to the scattering is given by $J_{Fl}(s)$ [15, 16]. The local density fluctuation can be obtained by extrapolation of the scattered intensity in this region to $\Theta = 0$. However, such an extrapolation can be only performed if further assumptions on the dependence of $J_{Fl}(s)$ on s are made, which lead to additional ambiguities. Therefore, similar to the procedures applied in earlier investigations [13, 14], in the present work $J_{Fl}(s)$ has been assumed to have a constant value J_{Fl} not dependent on s. This value is obtained by variation of J_{Fl} and d_z in a process demanding Porod's law to be fulfilled in a maximal interval of s. The variational process is explained in more detail below. Thus, the function $J_{Fl}(s)$ dealt with in this paper is just the constant smeared intensity value subtracted from the whole scattering curve in order to maximize the region in which Porod's law is valid. For the investigated sample series, this region was found to be approximately 0.1 $\text{nm}^{-1} < s < 0.2\ \text{nm}^{-1}$. Within this region J_{Fl} is determined with an accuracy better than 1%, which is need-

ed in order to obtain values of d_z with sufficient accuracy. The error in the whole region of s involved in this procedure is negligible for all evaluations in this paper except that of the electron density fluctuation. This is due to the following: For small values of s the background scattering is negligible and for larger values of s, up to infinity, the measured data are substituted by the value obtained by Porod's law.

In the determination of the electron density fluctuations, on the contrary, the substitution of the extrapolated value of $J_{Fl}(s)$ by the constant value at intermediate angles, J_{Fl}, may involve some error. Yet, it seems to us that this error is not larger than that involved in the procedures which use the extrapolation process.

The variational process by which J_{Fl} and d_z are determined is carried out in the following way:

a) The data are plotted in the Stein diagram [17] $\ln [s^3(J(s) - J_{Fl})]$ vs $s^{1.81}$, which is based on an approximation found empirically for the infinite-length slit smeared scattering for a model with Gaussian transition zone

$$(J(s) - J_{Fl}) \approx A_p/s^3 \exp(-38(\sigma_Z s)^{1.81}) . \quad (6)$$

σ_Z is the variance of the Gaussian transition zone, A_p is the Porod asymptote. The width of the transition zone, d_z, is then defined as $3\sigma_z$;

b) The value of J_{Fl} is then varied until the range in which the data follow a linear decrease is maximized;

c) A straight line is fitted to the data in this range. The values of the Porod asymptote A_p and of σ_z are obtained from the intercept and slope of the straight line, respectively;

d) With the parameters A_p, σ_z, and J_{Fl} obtained in this way, the interference function $\tilde{G}_{id}(s)$ of the ideal two-phase system is calculated from the measured scattering intensity $J(s)$ by the formula of Ruland

$$\tilde{G}_{id}(s) = (J(s) - J_{Fl})\, s^3 [(1 - 8\pi^2\sigma_z^2 s^2) \operatorname{erfc}(2\pi\sigma_z s) + 4\sqrt{\pi\sigma_z s} \exp(-4\pi^2\sigma_z^2 s^2)]^{-1} - A_p . \quad (7)$$

In contrast to Eq. (6), this formula is strictly valid and does not involve any approximation. If, at large values of s, the curve representing $\tilde{G}_{id}(s)$ is not parallel to the s-axis, the parameter σ_z is corrected with finer variations. Furthermore, the parameter A_p is adjusted so that $\tilde{G}_{id}(s)$ approaches zero for large values of s;

e) The scattering of the ideal two-phase system with sharp transitions between the two phases and a uniform electron density within each phase $J_{id}(s)$ is calculated from the evaluated $\tilde{G}_{id}(s)$ by means of Eq. (5).

For the further evaluation of J_{Fl} one has to take into account the smearing of the scattering by the slit. The assumption of a constant value of J_{Fl} simplifies the procedure of desmearing. One simply has to divide the fluctuation background J_{Fl} by the effective integral slit length (in the plane of registration) in reciprocal space, W_1

$$I_{Fl} = J_{Fl}/W_1 . \quad (8)$$

Thus, the fluctuation background is obtained in absolute units (electrons per volume). In the case of our instrumental setup, W_1 was found experimentally to be 2.01 nm^{-1}.

3. Experimental section

The base sample of our investigation was a linear SBS tri-block copolymer with M_n(PB) = 80 800 g/mole and, for each of the end blocks, M_n(PS) = 21 200 g/mole. The synthesis and characterization of this polymer is described in [1–3], where it is named $L-1$. This polymer was extended by a paraffinic oil (oil I), and low molecular weight polybutadiene (lithene PM) and an aromatic oil (oil III). The densities and some other properties of the extender oils are given in [1–3].

The samples were prepared by dissolving the polymer in toluene, then the oil was added. From the homogeneous solution obtained, polymer films of 0.8 mm thickness were spin cast.

Measurements were carried out using Ni-filtered Cu-K_α radiation, a Kratky-Compact-Camera and a proportional detector with energy discrimination. Several samples with the lateral dimensions of 1 × 5 cm were stacked to reach the optimal thickness. In order to determine the scattered intensity with the necessary accuracy, the samples were measured using two different entrance slits with vertical dimensions of 40 μm and 80 μm, respectively, in overlapping angular regions ($0.014\ nm^{-1} < s < 0.058\ nm^{-1}$ with 40 μm and $0.02\ nm^{-1} < s < 0.26\ nm^{-1}$ with 80 μm). The absorption factor and the primary beam power per unit slit length, P_o, were measured using the moving slit method [7]. Additionally, the "Lupolen Standard" method [6] was used to check P_o. The values determined by these two methods differ by less than 2%.

4. Results

4.1 Elementary analysis of the extender oils

To obtain the electron densities of the oils, an elementary analysis was performed using a CHNO-Halfmicro apparatus (Heraeus).

The results of the elementary analysis showed that more than 98 wt% of both oils consist of the two elements C and H. Neglecting the rest we computed the

C/H-ratio to be 1.90 for the paraffinic and 1.42 for the aromatic oil. This yields electron densities $\varrho_{el} = 296$ el/nm^3 for the paraffinic and 336 el/nm^3 for the aromatic oil, assuming mass densities of 0.8665 g/cm^3 for the paraffinic and 1.0096 g/cm^3 for the aromatic oil as measured. Compared to the electron densities of the two polymer phases, ϱ_{el} of the aromatic oil is close to the electron density of the pure PS sample (339 el/nm^3), and ϱ_{el} of the paraffinic oil lies near the electron density of the PB phase (301 el/nm^3). The latter one was computed from the composition and the density of the pure SBS sample ($\varrho_{SBS} = 0.946$ g/cm^3, 0 wt% oil), and from the density of the homopolymer PS ($\varrho_{PS} = 1.047$ g/cm^3).

The electron density of lithene PM is the same as that of PB, namely 301 el/nm^3.

4.2 SAXS measurements

In order to find out if some orientation is present in the material, the SAXS was measured in two different directions, namely parallel and perpendicular to the rotational axis of the spin casting apparatus. The results for the samples extended with 13 wt% of aromatic oil are represented in Fig. 1. A small difference is observed in the position of the peak (long period L), indicating that the samples are slightly oriented. Similar results were observed for the other samples. For internal coherence of the data, all results presented here were obtained by measuring in the direction of the rotational axis of the spin casting apparatus, where the long period is smaller.

In Fig. 2 a collection of typical scattering curves, obtained on pure SBS as well as on SBS extended with paraffinic and aromatic oil is presented. All samples show an intense scattering pattern with a long period L of about 47 nm, and a much weaker reflection corresponding to a peak position ratio of about $1:\sqrt{7}$. Small differences in the positions of the peaks as well as in the scattered intensities can be noticed. The results for the samples containing paraffinic oil and lithene PM respectively are similar.

The positions of the two peaks of each curve in Fig. 2, together with that of a smaller one with ratio $1:\sqrt{3}$ observed in the interference function, suggest a hexagonal packing of PS cylinders [18].

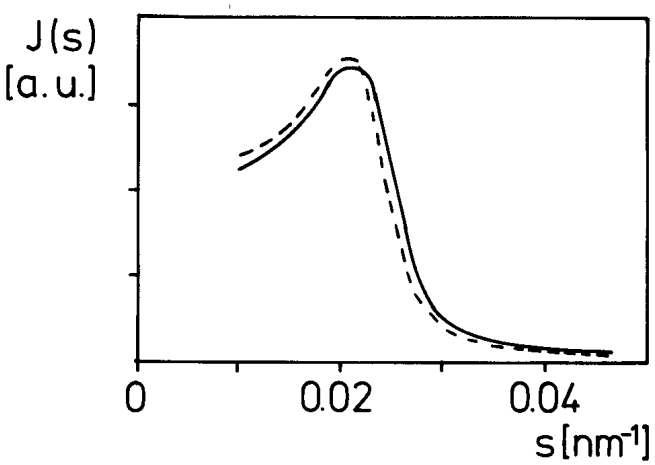

Fig. 1. SAXS curves of the SBS copolymer extended with 13 wt% of aromatic mineral oil. Effect of film orientation: dashed line; SAXS measured perpendicular to the rotational axis of the spin casting apparatus. Solid line: SAXS measured in the direction of the rotational axis

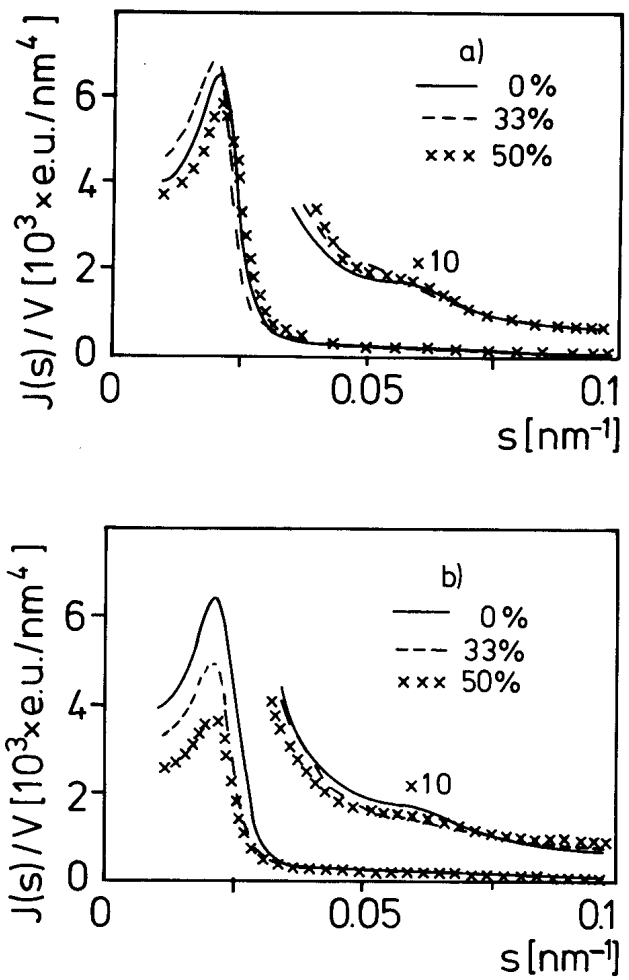

Fig. 2. Absolute SAXS curves for a SBS copolymer diluted with different weight amounts of a) paraffinic, and b) aromatic extender oil

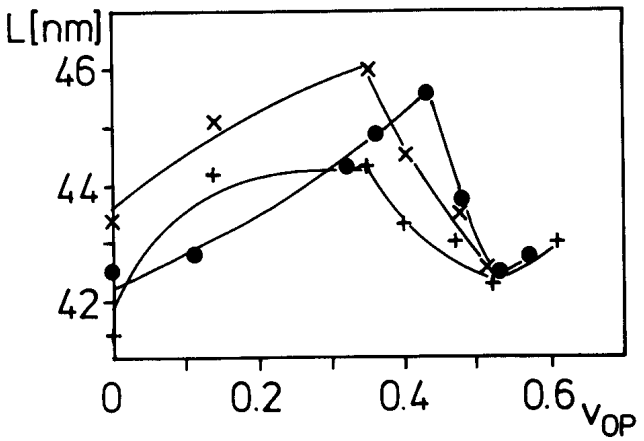

Fig. 3. Long period L of oil extended SBS copolymers as a function of v_{OP}, the volume fraction of oil in the polymer. (+) low molecular weight PB (lithene PM) as extender in oil; (×) paraffinic extender oil; (●) aromatic extender oil

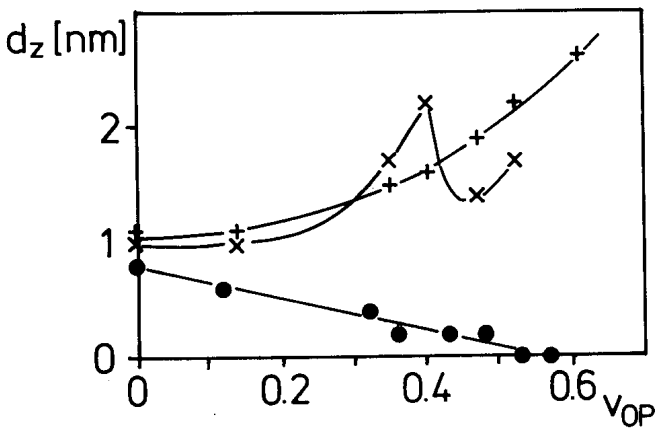

Fig. 4. Width d_z of the transition zone at the phase boundary of oil extended SBS copolymers as a function of v_{OP}, the volume fraction of oil in the polymer. (+) low molecular weight PB (lithene PM) as extender oil; (×) paraffinic extender oil; (●) aromatic extender oil

Figure 3 shows the long period L as a function of the volume fraction of oil in the polymer, v_{OP}. Additivity of the volumes is assumed when v_{OP} was calculated from the weight fractions. L was determined from the first maximum in the interference function $\tilde{G}_{id}(s)$. The determination of L directly from the intensities $J(s)$ results in slightly larger values of L while the features of the curves remain the same. With increasing oil content an increase of L is observed followed by a sudden decrease which indicates that some transition occurs. At the maximum of L, the measured value of L had only increased by a factor of 1.05 for aromatic and of 1.06 for paraffinic oil, while the volume had increased by a factor of 1.54 and 1.82, respectively.

Figure 4 shows the variation of the width of the phase boundary, d_z, as a function of the oil content. With J_{Fl} being determined with 1% reproducability, the value of d_z can be determined with an accuracy of $\pm$ 0.3 nm. It is interesting to note that d_z is decreased if aromatic oil is added, while it is increased by the addition of paraffinic oil or lithene.

The calculation of the scattering power Q_{id} yields the results represented in Table 1. Taking into account all the errors of determination, Q_{id} was determined with an error of 4%. It can be clearly recognized that blending with paraffinic oil does not change Q_{id}, while aromatic oil strongly decreases the scattering power. By means of Eq. (3) a value of $Q_{id} = 309$ (el/nm^3)^2 is obtained for an ideal two-phase system of pure PS and PB having a volume fraction of PS equal to 0.31 and the electron densities given in Section 4.1. The value of Q_{id} found experimentally (Eq. (2) with $J_{id}(s)$) is considerably smaller. This indicates that the phase separation between PS and PB is not complete. As the electron density of the aromatic oil is similar to that of the PS phase, the decrease of Q_{id} with increasing amount of aromatic oil can only be explained by assuming that the oil is mainly present in the PB phase, thus reducing the density difference $(\varrho_2 - \varrho_1)$ in Eq. (3). The electron density of the paraffinic oil and of lithene is the same as that of the PB phase. Therefore, the constant value of Q_{id} with increasing content of paraffinic and lithene oils indicates that these oils too are only entering the PB phase.

The electron density difference $\Delta\varrho$ was calculated from Q_{id} by means of Eq. (3) under the assumption that the oil is only present in the polybutadiene matrix

Table 1. Scattering power Q_{id}

Weigth fraction w_{OP} of oil in polymer	Scattering power Q_{id} [(el/nm^3)^2] for different types of extender oil		
	lithene PM	paraffinic oil	aromatic oil
0.0	116	118	121
0.13	99	110	117
0.33	106	118	87
0.38	113	117	70
0.44	107	121	76
0.50	96	114	69
0.55	–	–	65
0.58	89	–	57

and that the volumes simply add algebraically. If the assumption is accurate, the propagated error of determination can be estimated to be smaller than 0.6 el/nm^3. Figure 5 shows the results. $\Delta\varrho$ is represented as a function of the volume fraction of oil in the polymer, v_{OP}. In addition, in a second scale the corresponding volume fraction of the oil in the PB matrix, v_{OB}, is shown. Again it is assumed that the oil is present only in the polybutadiene matrix and that the volumes simply add algebraically. If the assumptions made were correct, and if one assumes that the difference of the theoretical and the experimental value of $\Delta\varrho$ is caused by the fact that the PB phase is contaminated by PS while the PS phase is pure, one would observe the relation between $\Delta\varrho$ and the oil content show by the dashed lines. Possible reasons for the deviations from these lines are discussed in the next section.

In Figs. 6 and 7 the segment length distributions, $n(r)$, normalized to the same height, are represented

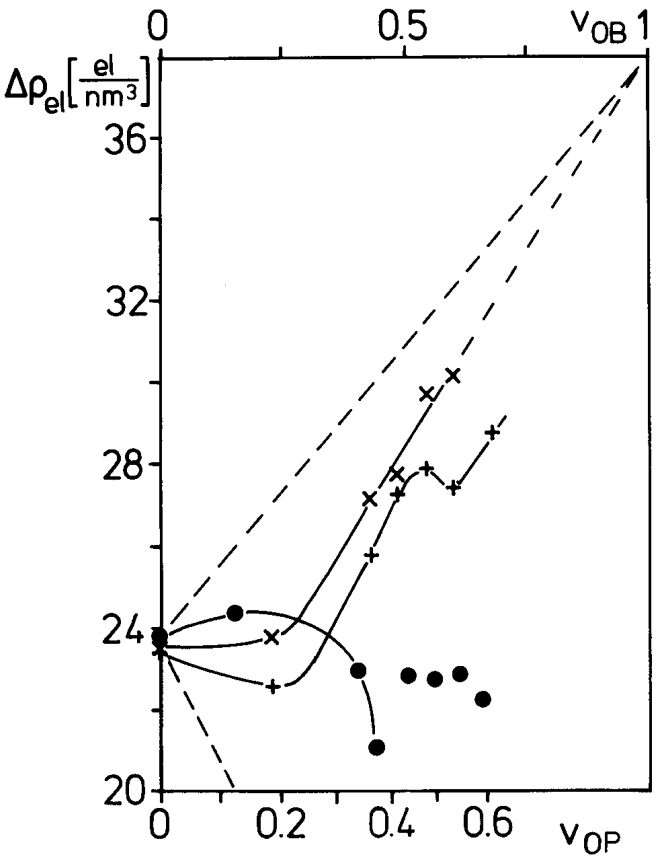

Fig. 5. Electron density difference $\Delta\varrho$ of oil extended SBS block copolymers as a function of v_{OP}, the volume fraction of oil blended into the polymer. v_{OB} = volume fraction of oil blended into the PB phase ($v_{OB} = 1$ corresponds to $v_{OP} = \infty$); (+) low molecular weight PB (lithene PM) as extender oil; (×) paraffinic extender oil; (●) aromatic extender oil

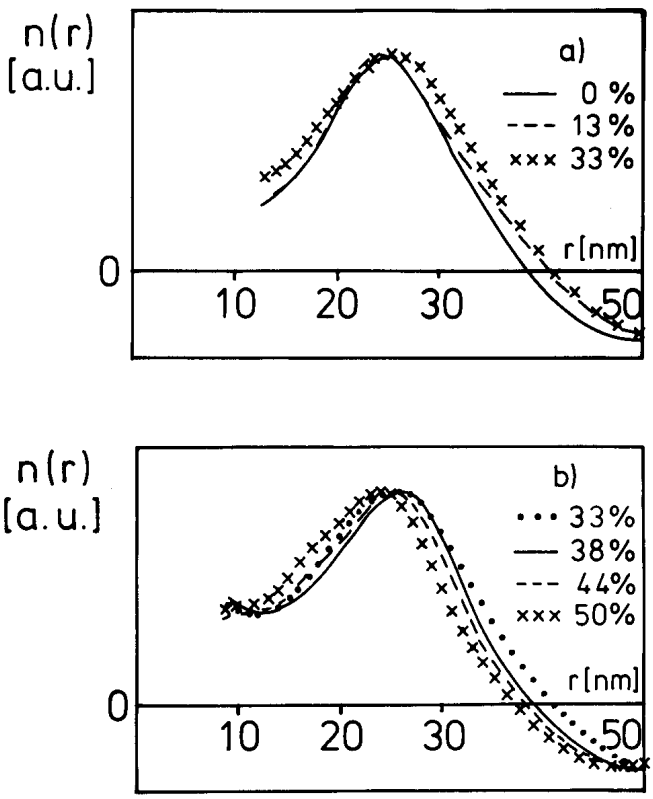

Fig. 6. Segment length distributions $n(r)$ for a SBS copolymer extended with paraffinic oil; a) low weight fractions of oil, b) high weight fractions of oil. The weight fractions of the oil are indicated in the figures

for samples containing different amounts of oil. For all the samples the position of the maximum of $n(r)$ is at about 25 nm. To a first approximation, this value could be considered to be the diameter of the polystyrene cylinders. As one can see, the dilution by oil causes changes in $n(r)$. The interpretation of this changes is discussed in the following section.

In Fig. 8 the density fluctuation I_{Fl}, as determined by the variational process described in the theoretical scection, is plotted as a function of the volume fraction of oil. The addition of lithene or paraffinic oil does not alter the fluctuations on a rough scale, while that of aromatic oil considerably increases them.

5. Discussion

5.1 Dimensions and shape of the domains

Previous investigations suggest that in the case of the composition of our undiluted sample cast from toluene the PS domains form cylinders [4, 5]. For the

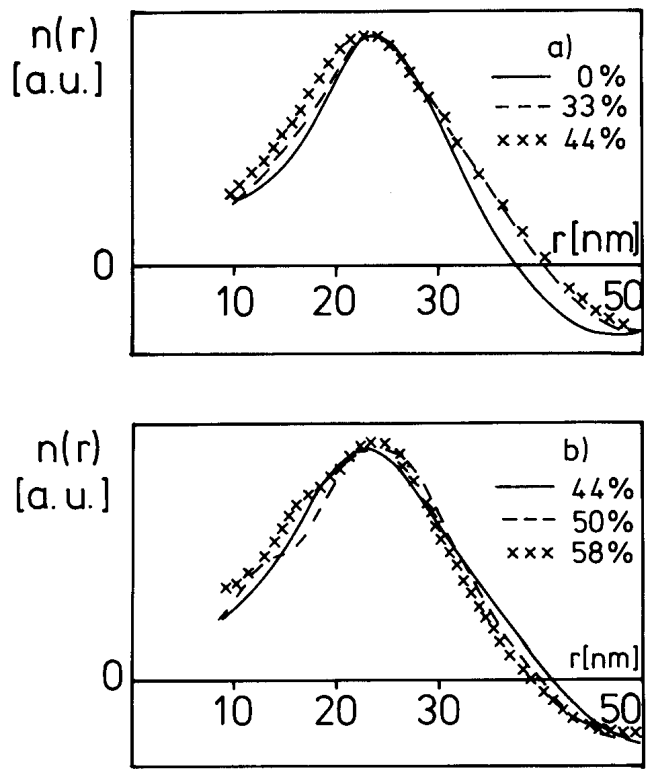

Fig. 7. Segment length distributions $n(r)$ for a SBS copolymer diluted with aromatic oil; a) medium weight fractions and b) high weight fractions of oil

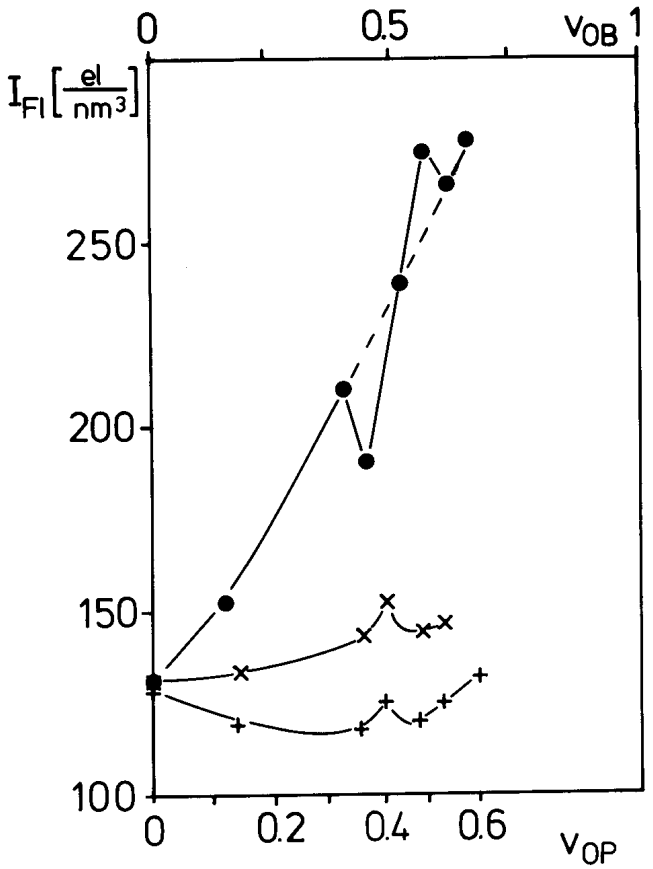

Fig. 8. Density fluctuation background I_{FI} of oil-extended SBS copolymers as a function of v_{OP}, the volume fraction of oil blended into the polymer. v_{OB} = volume fraction of oil blended into the PB phase; (+) = low molecular weight PB (lithene PM) as extender oil; (×) = paraffinic extender oil; (●) = aromatic extender oil

undiluted sample, the lateral center-to-center distance between cylinders obtained from the long period is about 43 nm. As the segment length distribution $n(r)$ has only one maximum, (see Figs. 6 and 7), the average thickness of the PS cylinders should be of the same order as that of the PB regions between the cylinders. Therefore, both regions have a thickness of about 25 nm.

This work, as well as a SANS study [19] shows that the oil enters mainly the PB phase. Therefore, if we assume additivity of volumes the average distance between the cylinders should increase with increasing oil content. Such an increase is observed (see Fig. 3), however, it is not as large as it should be. For example, if the volume increases by a factor of 1.5 (the value at which the maximum of L is observed in case of paraffinic oil), L should increase by a factor of $(1.5)^{1/2} = 1.22$, while the measured value of L is only increased by a factor of 1.06. Such a result is inconsistent with the assumption of cylinders of infinite length. Obviously, the cylinders have a finite length, and the length decreases with increasing oil content. In addition, it is possible that the swelling is not isotropic: the distance between the cylinders in longitudinal direction, which is not measured by L, may increase stronger than that in lateral direction [20].

After a critical amount of oil is reached ($v_{OP} = 0.33$ for paraffinic oil and lithene, $v_{OP} = 0.43$ for aromatic oil) L decreases strongly. We think that this is an indication for a transition in the morphology, i.e., a change of the form of the PS domains from cylinders to spheres. This is in agreement with conclusions based on mechanical investigations [1–3].

Such a conclusion is also supported by the segment length distribution $n(r)$. As a consequence of the addition of up to 33 wt% paraffinic oil to the polymer, the righthand side of the original peak grows (Fig. 6a). This indicates that blending with small amounts of paraffinic oil leads to an expansion of the PB and PS domains. If the oil content exceeds 33 wt% (Fig. 6b)

the relative number of the long segments seems to decrease continously with increasing amount of paraffinic oil. In addition, on the lefthand side of the observed peak, a shoulder grows and the peak shifts to smaller distances. Apparently, the PS domains become smaller in agreement with the measured long period.

Thus we can distinguish two distinct states of the superstructure while blending the polymer with increasing amounts of paraffinic oil: a) a growth of the superstructure, and b) a reduction of domain sizes associated with the change from cylindrical to spherical PS domains.

In the case of aromatic oil (Fig. 7a), the main effect is more a broadening of the first peak than a growing of the lefthand side of this peak. This could be ascribed to a smearing out of the superstructure caused by a broadening of the distribution of domain sizes. The three samples containing 50% or more oil (Fig. 7b) show segment length distributions similar to those found for parafinic oil with oil contents larger than 33%: the growth of a shoulder at the left side of the peak and a relative decrease of longer segments. These three samples are in the region of oil dilution where, according to mechanical investigations [1–3], the morphological transition is supposed to take place. Thus, in the case of adding increasing amounts of aromatic oil we can distinguish the following two states of structural changes: a) smearing out of the initial superstructure, and b) reduction of domain sizes.

5.2 *Local density fluctuations* I_{Fl}

The almost constant value of I_{Fl} (see Fig. 8) for the samples extended with paraffinic oil clearly demonstrates that this type of oil fills the PB phase of the polymer. If the oil entered the PS phase, the incompatibility between this oil and PS, together with the difference of the electron density of the oil and the PS, would considerably increase the inhomogeneity of this phase, hence raising the fluctuation background.

The increase of I_{Fl} with increasing amount of aromatic oil is in agreement with our conclusion that this oil enters the PB phase. As this oil is more compatible with PS, its presence in this phase would not increase I_{Fl} as observed.

It is interesting to note that at the critical concentration at which the morphological transition occurs, a larger increase followed by a drop in the local electron density fluctuation is observed in each of the three curves (see Fig. 8). One may speculate that the increasing distance of the PS cylinders caused by an increasing oil content is accompanied by an increase of internal stress due to the elongation of the PB chains. This stress increase may promote a preliminary step of phase separation resulting in an increase of the fluctuations. As a consequence of the change of the morphology, the stress is reduced and the local electron density fluctuations become smaller again.

The decrease of I_{Fl} occurring when the content of aromatic oil in PB is increased from 0.48 to 0.5 may be explained by the formation of small droplets of oil within pores in the polymer. However, another assumption would also be able to explain this fluctuation breakdown: At this point a significant amount of aromatic oil might begin to mix with the PS phase, where it causes weaker density fluctuations due to its better compatibility with this phase.

5.3 *Thickness* d_z *of the phase boundary zone*

The parameter d_z, characterizing the width of the phase boundary, is increased by diluting the polymer by paraffinic oil, while it is decreased by diluting by aromatic oil (see Fig. 4). Obviously, the paraffinic oil is widening the phase transition region and the aromatic oil leads to a decrease of this zone. However, in the case of the aromatic oil the large local phase density fluctuations lower the significance of the value of d_z because the phase transition zone vanishes in the statistical noise of the local density fluctuations.

5.4 *Electron density difference* $\Delta\varrho$

For the undiluted polymer a value of $\Delta\varrho$ of 24 el/nm^3 is obtained, if it is assumed that the volume fraction of the PS phase, v_{PS}, is given by 0.31, as calculated from the weight fraction. This measured $\Delta\varrho$ is far below the theoretical value that can be computed from the electron densities of pure PS and PB (38 el/nm^3). So the data show that the initial SBS block copolymer cannot be treated as an undisturbed system, in which both phases behave like pure PS and PB.

Within the frame of a two-phase model, two physical causes may be invoked to explain such a result:

a) A variation of the volume fractions of the two phases due to internal stresses caused by their incompatibility. A larger v_{PS} would lead to smaller electron density ϱ_{PS} and, in order to maintain the measured SBS mass density, to a higher ϱ_{PB}. In Eq. (3) this would lead to a small increase of the value of $v_{PS}(1-v_{PS})$, while the term $(\varrho_{PS}-\varrho_{PB})^2$ would be reasonably lowered;

b) Contamination of one phase by the other due to incomplete phase separation. This would lead to an approach of the mean electron densities of the two phases.

If one assumes a pure PB phase and a mixed PS/PB phase, one finds that 23 vol % of PB is present in the PS domains, but if one has a pure PS phase, then 16 vol % of PS is present in the PB domains.

In addition, the presence of interstitial spaces (pores) could also cause deviations from the theoretical value supplied by Eq. (3). In this case, the two-phase model would not be valid anymore.

In the case of complete separation of PS and PB in two undisturbed pure phases, because of the similar electron densities of the two substances a dilution of PB with our paraffinic oil should only cause little change in $\Delta\varrho$ (+ 5 el/nm^3). Yet, as discussed above, the electron densities of the two phases are not those of the ideal case. If we assume that, in the undiluted polymer, we have a pure PS phase and a PB phase contaminated by PS, $\Delta\varrho$ would increase as shown by the dashed lines in Fig. 5. The experimental data show a linear increase of $\Delta\varrho$ with the oil concentration of the PB phase after an initial almost constant value. The linear increase tends towards the computed theoretical value. This suggests that paraffinic oil dilution reduces the interactions between the rubber and the rigid phase, allowing the PS and PB domains to achieve a better phase separation and/or to relax to their usual density.

The initial almost constant value of $\Delta\varrho$ indicates that the assumption of simple algebraic additivity of volumes does not hold for such small concentrations of oil: small amounts of oil probably enter some pores present in the polymer.

The dilution of the PB matrix by aromatic oil should lead to a strong decrease of $\Delta\varrho$, because this oil has a larger electron density than the matrix phase. The behavior actually observed is rather complicated. At low oil concentrations an almost constant value is obtained, similar to the dilution by paraffinic oil. This effect can be ascribed to a violation of volume additivity of the mixed matrix phase which might be caused by the incompatibility of PB and the aromatic oil. For higher oil concentrations $\Delta\varrho$ strongly decreases, as theoretically predicted. This however is only true for values of v_{OB} up to approximately 0.7. If the oil content becomes larger, $\Delta\varrho$ suddenly increases again remaining then almost constant. In this region of concentration, we think that either part of the aromatic oil enters the rigid phase or that it forms small droplets in the PB phase. In both cases $\Delta\varrho$ and v_{OB} are not correctly determined which, as one can show, leads to the unexpected increase of the apparent value of $\Delta\varrho$.

Appendix: Derivation of Eq. (1)

Let us assume that the primary beam is of rectangular shape having the dimensions H_s and L_s on the sample and H_r and L_r in the plane of registration respectively (see Fig. 9). The dimensions of the rectangular slit of the counter are denoted by H_c and L_c. The distance between the slit of the counter and the primary beam is designated by m. According to the formula valid for point collimation [21, 22], the partial power dP scattered from the volume element $t \cdot d\sigma_s$ of the sample with thickness t into the area $d\sigma_c$ of the slit of the detector is given by

$$dP = i_0 \cdot t\, d\sigma_s \cdot \frac{r_e^2}{r^2} \cdot f_P \cdot e^{-\mu t} \cdot i_{dV}(\vec{s})\, d\sigma_c\,, \quad \text{(A-1)}$$

i_0 being the intensity of the primary beam, f_P the polarization factor, r_e the classical electron radius, r the

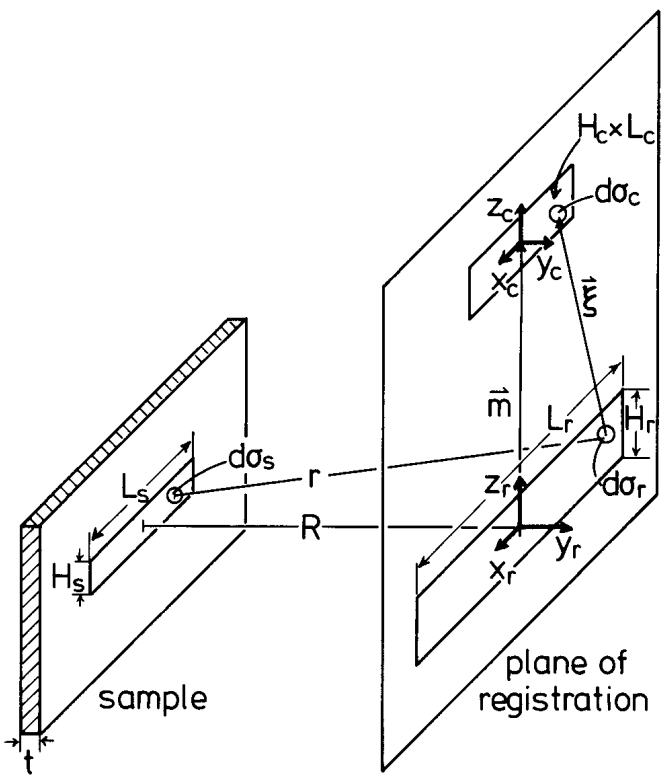

Fig. 9. Nomenclature and geometrical relations between sample and plane of registration for a small angle x-ray camera with slit collimation

distance between $d\sigma_s$ and $d\sigma_c$, $dV = t\,d\sigma_s$ the volume irradiated by the partial primary beam, and $i_{dV}(\vec{s})$ the Fourier transform of the convolution product of the electron density $\Delta\varrho^{*2}(\vec{r})$ integrated over dV

$$i_{dV}(\vec{s}) = \frac{i(\vec{s})}{dV} = \frac{1}{dV}\int_{dV} \Delta\varrho^{*2}(\vec{r}) \cdot e^{2\pi i \vec{r}\vec{s}} d^3r\,. \quad \text{(A-2)}$$

The scattering vector $\vec{s}$ is defined by

$$|\vec{s}| = \frac{2\sin\theta}{\lambda}$$

2θ being the scattering angle and λ the wavelength of the radiation.

In the tangent plane approximation $\vec{s}$ is related to the vector $\vec{\xi}$ in Fig. 9 by the equation

$$\vec{s} = \frac{\vec{\xi}}{\lambda \cdot r}\,. \quad \text{(A-3)}$$

In order to express $\vec{s}$, $d\sigma_s$ and $d\sigma_c$ by the same coordinates we introduce two coordinate systems x_r, z_r and x_c, z_c in the image of the primary beam and in the slit of the detector respectively (see Fig. 9). The two components of the vector $\vec{\xi}$ are then given by

$$\xi_x = x_c - x_r\,; \quad \xi_z = m + z_c - z_r\,. \quad \text{(A-4)}$$

After replacing $d\sigma_s$ by its image in the plane of registration $d\sigma_r$, taking into account the corresponding affine transformation, we obtain

$$d\sigma_s = \frac{H_s \cdot L_s}{H_r \cdot L_r} \cdot d\sigma_r = \frac{H_s \cdot L_s}{H_r \cdot L_r} \cdot dx_r\,dz_r\,. \quad \text{(A-5)}$$

Furthermore,

$$d\sigma_c = dx_c\,dz_c\,. \quad \text{(A-6)}$$

Finally, as a consequence of the small scattering angle we can approximate the slightly varying distance r by the constant distance R between the plane of the sample and that of registration. In the same way f_p can be approximated by 1.

By integration over the sample as well as over the slit of the detector we then obtain the total scattered power measured by the detector in the position m

$$P = i_0\,t\,e^{-\mu t}\,\frac{r_e^2}{R^2}\,\frac{H_s\,L_s}{H_r\,L_r} \cdot \int\int i_{dV}(\vec{s})\; Y_{L_r}(x_r)\,Y_{H_r}(z_r)\,Y_{L_c}(x_c)\,Y_{H_c}(z_c)\,d\sigma_r\,d\sigma_c \quad \text{(A-7)}$$

with the shape functions Y being defined as

$$Y_L(x) := \begin{cases} 1 \text{ for } |x| \le L/2 \\ 0 \text{ for } |x| > L/2 \end{cases}. \quad \text{(A-8)}$$

As both H_r and H_c are small, we can neglect the dependence of $i_{dV}(\vec{s})$ on z_r and z_c. The integration over dz_c and dz_r thus yields $H_r \cdot H_c$ and we obtain, considering that $H_s L_s t = V$, the irradiated volume of the sample

$$P = i_0\,e^{-\mu t}\,\frac{r_e^2}{R^2}\,\frac{H_c}{L_r}\,V \times \int_{-\infty}^{\infty}\int_{-\infty}^{\infty} i_{dV}(\vec{s})\,Y_{L_r}(x_r)\,Y_{L_c}(x_c)\,dx_r\,dx_s\,. \quad \text{(A-9)}$$

Further, we transform the variables x_r, x_c to $x_r, \xi_x = x_r - x_c$. At last we take into account that, according to the approximation $\xi_z \approx m$ together with Eqs. (A-3) and (A-4), $\vec{s}$ only depends on ξ_x and m. Thus we obtain

$$\begin{aligned} &\int_{-\infty}^{\infty}\int_{-\infty}^{\infty} i_{dV}(\vec{s})\,Y_{L_c}(x_c)\,Y_{L_r}(x_r)\,dx_c\,dx_r \\ &= \int_{-\infty}^{\infty}\int_{-\infty}^{\infty} i_{dV}(\xi_x, m)\,Y_{L_c}(x_c)\,Y_{L_r}(x_r)\,dx_c\,dx_r \\ &= \int_{-\infty}^{\infty} i_{dV}(\xi_x, m) \int_{-\infty}^{\infty} Y_{L_c}(x_r - \xi_x)\,Y_{L_r}(x_r)\,dx_r\,d\xi_x \\ &= L_c \int_{-\infty}^{\infty} i_{dV}(\xi_x, m)\,W(\xi_x)\,d\xi_x \end{aligned} \quad \text{(A-10)}$$

with

$$W(\xi_x) = \frac{1}{L_c}\int_{-\infty}^{\infty} Y_{L_c}(x_r - \xi_x) \cdot Y_{L_r}(x_r)\,dx_r\,. \quad \text{(A-11)}$$

$W(\xi_x)$ is the effective weight function of the primary beam in the direction of the slit length. It is normalized to $W(0) = 1$.

We now transform into the reciprocal space with the coordinates $s_1 = \frac{\xi_x}{\lambda \cdot R}$ and $s_3 = \frac{m}{\lambda \cdot R}$ using the relation $d\xi_x = \lambda R\,ds_1$ and obtain P as a function of s_3

$$P(s_3) = i_0 \cdot e^{-\mu t} \cdot \frac{r_e^2}{R^2}\,\lambda \cdot \frac{H_c \cdot L_c}{L_r} \cdot j(s_3) \quad \text{(A-12)}$$

with

$$j(s_3) = V \cdot \int i_{dV}(s_1, s_3) \cdot W(s_1)\, ds_1 \qquad \text{(A-13)}$$

being the smeared absolute intensity.

By using the moving slit device, the primary beam power per unit length of the slit, P_0', is measured. From this quantity i_0 can be calculated

$$i_0 = \frac{P_0' \cdot L_r}{H_s \cdot L_s}. \qquad \text{(A-14)}$$

Inserting this into Eq. (A-12) and solving the latter equation for $j(s_3)/V$ one obtains Eq. (1) after identifying s in Eq. (1) with s_3 in this appendix and j with J.

References

1. Bordeianu R, Cerchez I, Ghioca P, Stancu R, Buzdugan E (1986) In: Ceausescu E (ed) Forschungen im Bereich der Chemie und Technologie der Polymere. Birkhäuser, Basel, pp 73–75
2. Ceausescu E, Bordeianu R, Ghioca P, Buzdugan E, Stancu R, Cerchez I (1984) Pure & Appl Chem 56:319
3. Ceausescu E, Bordeianu R, Ghioca P, Cerchez I, Buzdugan E, Stancu R (1983) Rev Roumaine Chem 28:299
4. Folkes MJ, Keller A (1973) In: Haward RN (ed) The Physics of glassy Polymers. Applied Science Publishers, London
5. Noshay A, McGrath J (1977) Block Copolymers. Academic Press, New York
6. Kratky O, Pilz I, Schmitz J (1966) Colloid Interface Sci 21:24
7. Stabinger H, Kratky O (1978) Makromol Chem 179:1655
8. Mering J, Tchoubar-Vallat D (1966) CR Acad Sci Paris 264:1703
9. Mering J, Tchoubar D (1968) J Appl Cryst 1:153
10. Perret R, Ruland W (1968) J Appl Cryst 1:308
11. Ruland W (1971) J Appl Cryst 4:70
12. Stribeck N, Ruland W (1978) J Appl Cryst 11:535
13. Stribeck N (1980) Dissertation, Marburg
14. Siemann U, Ruland W (1982) Colloid Polym Sci 260:999
15. Wendorff JH, Fischer EW (1973) Koll Z u Z Polym 251:876
16. Rathje J, Ruland W (1976) Colloid Polym Sci 254:358
17. Koberstein JT, Morra B, Stein RS (1980) J Appl Cryst 13:34
18. Luzzati V, Mustachi H, Skoulios A, Husson F (1960) Acta Cryst 13:660
19. Pringle OA (1981) Dissertation, University of Missouri-Columbia
20. Polizzi S, Stribeck N, Zachmann HG, Bordeianu R (1988) Polymer Composites 9:in press
21. Kratky O, Porod G, Kahovec L (1951) Z f Elektrochem 55:53
22. Perret R, Ruland W (1971) J Appl Cryst 5:116

Received June 10, 1988;
accepted October 25, 1988

Authors' address:

Prof. Dr. H. G. Zachmann
Institut für Technische und Makromolekulare Chemie
Bundesstr. 45
D-2000 Hamburg 13, F.R.G.